

DOI: 10.17617/2.3195750

*Proceedings of the 9th Solar Polarization Workshop SPW9*

A workshop held in Göttingen, Germany, from August 26 to August 30, 2019

Achim Gandorfer, Andreas Lagg, Kerstin Raab (eds.)

© The author(s) 2019. Published open access by MPS 2020

# The "Second Solar Spectrum" of the post-AGB binary 89 Herculis.

M. Gangi<sup>1,\*</sup> and F. Leone<sup>2</sup>

<sup>1</sup>INAF - Osservatorio Astrofisico di Catania, Via S. Sofia 78, I-95123 Catania, Italy

<sup>2</sup>Università di Catania, Dipartimento di Fisica e Astronomia, Sezione Astrofisica Via S. Sofia 78, I-95123 Catania, Italy

\*currently at: INAF - Osservatorio Astronomico di Roma, Via Frascati 33, I-00078 Monte Porzio Catone, Italy. Email: manuele.gangi@inaf.it

**Abstract.** We report a spectropolarimetric study of the post-AGB binary system 89 Herculis, based on data acquired with the high-resolution Catania Astrophysical Observatory Spectropolarimeter, the HARPS-North Polarimeter and the Echelle Spectropolarimetric Device for the Observation of Stars.

The linear polarization clearly detected across single atmospheric lines in absorption is characterized by complex Q and U morphologies that are variable with the orbital period of the system. Gauss-level magnetic fields, continuum depolarization due to pulsations, hot spots and scattering in the circumstellar environment were excluded as possible origin of the observed polarization.

In the context of the optical pumping mechanism, we suggest that the anisotropy of the stellar radiation field, fuelled by the close binary companion, can be responsible of the observed periodic properties of the spectral line polarization.

We conclude that high resolution linear spectropolarimetry could be an important diagnostic tool in the study of aspherical envelopes of cool and evolved stars.

## 1 Introduction

In stellar astrophysics, high resolution linear spectropolarimetry is considered as a promising searching tool for a variety of environments. Despite the difficulties involved in data acquisition and interpretation, it deserves to be a standard observational technique. Indeed, different spectropolarimetric studies have been carried out on evolved stars like the Mira  $\chi$  Cygni (Lèbre et al. 2014; López Ariste et al. 2019) and the red supergiant Betelgeuse (Aurière et al. 2016; López Ariste et al. 2018). In analogy to the linearly polarized spectrum of the Sun (the so-called *Second Solar Spectrum*, Ivanov 1991) it appears that evolved stars can be characterized by the presence of polarization signals across spectral lines. In this context we focused on the polarimetric properties of the post-AGB 89 Herculis.

89 Herculis is considered a prototype of post-AGB binaries with circumbinary disk. This F-type star has an orbital period of about 288 days (Waters et al. 1993) and pulsates in 63 days (Arellano Ferro 1984). Due to the strong mass loss from the primary star, there are two nebular components: an hour-glass structure and an unresolved circumbinary Keplerian disk (Bujarrabal et al. 2007).

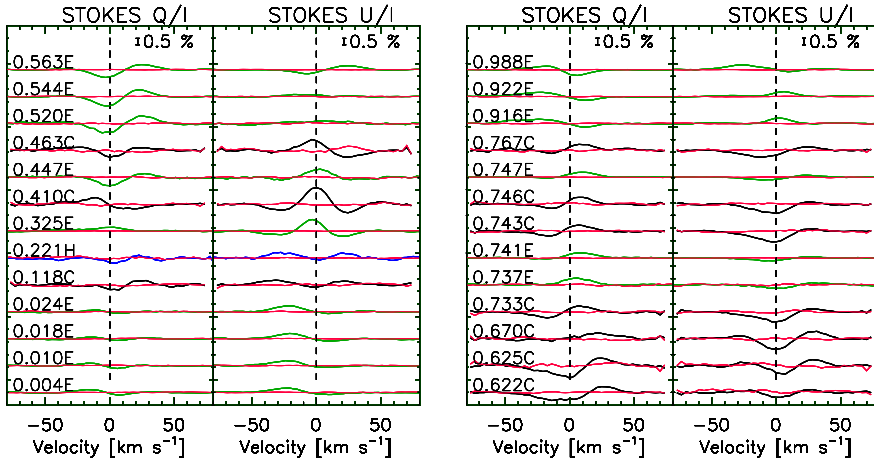


**Figure 1.** LSD Stokes Q/I and U/I profiles of 89 Her, vertically shifted for better visualization according to the orbital phase. The corresponding null spectra are shown in red. The null spectra (Leone et al. 2016a) check for the presence of any spurious contribution to the polarized spectra and errors in the data reduction process. 'E': ESPaDOnS; 'C': CAOS; 'H': HANPO.

## 2 Observational data

We undertaken a spectropolarimetric observational campaign using the high-resolution Catania Astrophysical Observatory Spectropolarimeter (CAOS:  $R=55000$ , Leone et al. 2016a) and the HARps-North Polarimeter (HANPO:  $R=115000$ , Leone et al. 2016b). Data were reduced and Stokes Q/I and U/I spectra extracted according to Leone et al. (2016a). Further data, acquired with the Echelle SpectroPolarimetric Device for the Observation of Stars (ESPaDOnS:  $R=68000$ , Donati et al. 2006) were retrieved from the Canadian Astronomy Data Centre. A total of 26 spectra, covering the full orbital period of the sytem, has been obtained.

Despite the photon noise, we have found that the ESPaDOnS Q/I and U/I spectra present not-null signals, that are clearly visible across individual photospheric lines. An Atlas of such spectra is reported in Gangi & Leone (2019). Due to the lower resolution, in CAOS spectra we did not found any direct evidence of polarization. For this reason we applied the multi-line LSD technique (Donati et al. 1997) to computed, for each observational date, a very high ( $10^3 - 10^4$ ) signal-to-noise ratio (SNr) I, Q/I and U/I profile. We have first constructed the line mask from a synthetic spectrum computed by SYNTHE (Kurucz 2005) with stellar parameters given in Waters et al. (1993). Spectral region was chosen between  $4250 \text{ \AA}$  and  $8000 \text{ \AA}$ . Lines weaker than the noise level were excluded, as well as specific elements like H, Ca I, Na I and telluric lines. A set of about 1000 spectral lines was then selected for the calculation. Further details about the LSD computation are in Leone et al. (2018). The obtained LSD profiles show complex Q/I and U/I morphologies variable in time (Fig. 1).

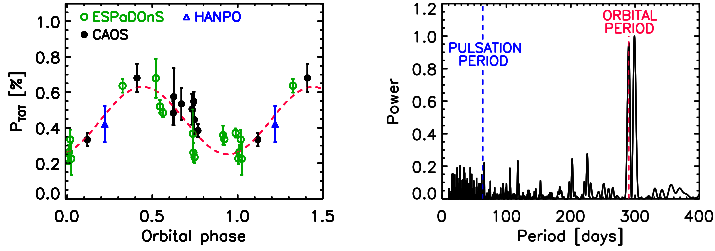


**Figure 2.** Left: Total LSD polarization  $P = \int \sqrt{(Q/I)^2 + (U/I)^2} d\lambda$  folded with the orbital phase. The latter was computed according to the following ephemeris:  $JD = 2446013.72(\pm 16.95) + 288.36(\pm 0.71)$  days (Waters et al. 1993); a sine fit of variability is also shown. Right: the Lomb-Scargle (Scargle 1982) periodogram of  $P$  rules out a possible variability with the pulsation period of 89 Her.

### 3 Origin of polarization

Spectral lines in absorption with linearly polarized profiles are not common and different phenomena can potentially contribute to the polarization. To find out the mechanisms compatible with our data, we summarize here the main properties of the observed polarization:

- Temporal variability: the polarization degree measured across the LSD profile of 89 Herculis is variable with the orbital period, while no statistically relevant variability with the pulsation period is found (Fig. 2);
- Wavelength dependence: the polarization degree of 89 Her is independent of wavelength (Fig. 3);
- Circular polarization: 89 Her is a circularly unpolarized source (Sabin et al. 2015). We confirmed this result with new CAOS measurements.

In addition, using broad-band optical photopolarimetry, Akras et al. (2017) has found that the continuum flux of 89 Herculis is unpolarized.

From this, we exclude Gauss-level magnetic fields, continuum polarization due to pulsations, hot spots and scattering in the circumstellar environment as the possible origin of the observed polarization.

### 4 A possible mechanism: the optical pumping model

Most of the properties of the linearly polarized spectrum of the Sun (Stenflo & Keller 1997) are considerably influenced by the so-called optical pumping mechanism (Landi Degl’Innocenti 1998). This mechanism is based on the presence of an anisotropic radiation pumping process, which induce population imbalance between atomic sublevels (e.g., Trujillo Bueno, & Landi Degl’Innocenti 1997).

In 89 Her, the very close (0.31 AU, Bujarrabal et al. 2007) companion star can be responsible for an anisotropy in the total radiation field of the system. Atoms can be then radiatively

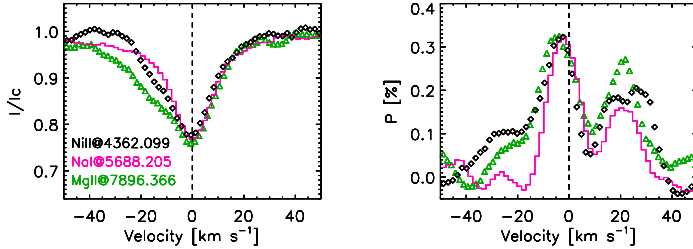


**Figure 3.** Examples of spectral lines with equal depth in different spectral regions (left) showing that, within the errors, polarization does not depend on wavelength (right).

aligned along the direction of anisotropy, i.e. the primary-secondary direction, which in turn can explain the observed variability with the orbital period.

To numerically explore this possibility we have first computed the anisotropy factor  $\omega$  (Landi Degl’Innocenti & Landolfi 2004), which is zero for an isotropic radiation field and 1 for an unidirectional radiation beam. Considering the photospheric and orbital parameters given in Waters et al. (1993) and Bujarrabal et al. (2007), we have found  $\omega \sim 0.8$ , that is compatible with the presence of a non-isotropic field between the two components of 89 Her.

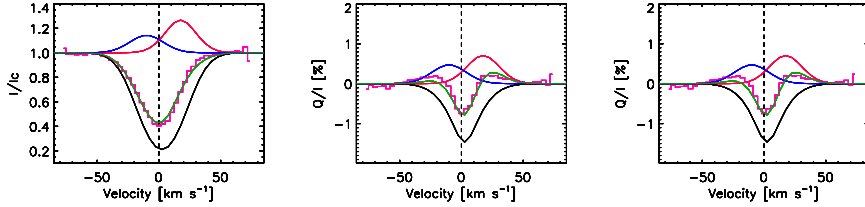
We have then used the HAZEL code (Asensio Ramos et al. 2008) to reproduce the observed Stokes profiles; computation details are in Leone et al. (2018). We have found that, for each profile, three components are required to fit the Stokes morphologies: a stationary feature in absorption (hereafter COMPONENT 2) and two oppositely Doppler-shifted components, the blue-shifted COMPONENT 1 and the red-shifted COMPONENT 3 (Fig. 4).

Fig. 5 shows the behaviour of the polarization angle  $\gamma$  of the three components derived from the HAZEL fit. The well defined saw-tooth variation of the  $\gamma$  angle, due to its definition in the  $[0, 180^\circ]$  range, is indicative of a closed loop of the polarization vector along the orbital motion of the secondary star. Furthermore, the longitude of periastron  $\omega = 395.3^\circ$  (Waters et al. 1993) implies that the polarization vector is north-south oriented ( $\gamma = 0^\circ$ ) in conjunctions (i.e. at phases  $\phi = 0.5, 1.0$ ) and east-west oriented ( $\gamma = 90^\circ$ ) in quadrature (i.e. at phases  $\phi = 0.25, 0.75$ ).

## 5 Discussion and conclusions

We have found that the optical pumping mechanisms can be at the origin of the observed linear polarization in the post-AGB binary 89 Her. The radiation field anisotropy, which is necessary for the operation of such process, may have origin in the close orbiting star.

We can qualitatively explain the behaviour of the Stokes morphologies considering the COMPONENT 2 representative of the average optical and physical properties of the primary component in reflecting and reprocessing radiation from the secondary star, while the blue-shifted COMPONENT 1 and red-shifted COMPONENT 3 represent the jet pointing towards us and the receding jet respectively.



**Figure 4.** Example of CAOS-LSD profile (pink) fitted with the HAZEL code. The solid (green) continuum is the sum the three components (blue, red and black continuum).

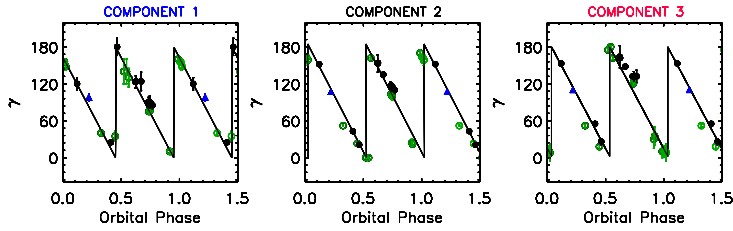


**Figure 5.** HAZEL polarization angles of the line components best matching the Stokes LSD profiles phase-folded with the orbital period. Symbols are as in Fig. 2.

This result shows how evolved stars can be characterized by a *Second Solar Spectrum*-like behaviour and gives us new instrument for better understanding the physical mechanisms underlying these kind of systems.

**Acknowledgements.** This study is based on observations made with the Catania Astrophysical Observatory Spectropolarimeter (CAOS) operated by the Catania Astrophysical Observatory.

I wish to express my gratitude to Dr. C. Scalia for his support during observations.

## References

- Akras, S., Ramírez Vélez, J. C., Nanouris, N., et al. 2017, MNRAS, 466, 2948
- Aurière, M., López Ariste, A., Mathias, P., et al. 2016, A&A, 591, A119
- Arellano Ferro, A. 1984, PASP, 96, 641
- Asensio Ramos, A., Trujillo Bueno, J., & Landi Degl’Innocenti, E. 2008, ApJ, 683, 542
- Bujarrabal, V., van Winckel, H., Neri, R., et al. 2007, A&A, 468, L45
- Donati, J.-F., Semel, M., Carter, B. D., et al. 1997, MNRAS, 291, 658
- Donati, J.-F., Catala, C., Landstreet, J. D., et al. 2006, Solar Polarization 4, 362
- Gangi, M., & Leone, F. 2019, Astronomische Nachrichten, 340, 409
- Ivanov, V. V., 1991, in NATO ASI Ser. C341, Stellar Atmospheres: Beyond Classical Models, ed. L. Crivellari, I. Hubeny & D. G. Hummer (Dordrecht: Kluwer), 81
- Kurucz, R. L. 2005, Memorie della Societa Astronomica Italiana Supplementi, 8, 189

- Landi Degl'Innocenti, E., & Landolfi, M. 2004, *Astrophysics and Space Science Library*
- Landi Degl'Innocenti, E., 1998, *Nature*, 392, 256
- Lèbre, A., Aurière, M., Fabas, N., et al. 2014, *A&A*, 561, A85
- Leone, F., Avila, G., Bellassai, G., et al. 2016, *ApJ*, 151, 116
- Leone, F., Cecconi, M., Cosentino, R., et al. 2016, *SPIE*, 99087K
- Leone, F., Gangi, M., Giarrusso, M., et al. 2018, *MNRAS*, 480, 1656
- López Ariste, A., Mathias, P., Tessore, B., et al. 2018, *A&A*, 620, A199
- López Ariste, A., Tessore, B., Carlin, E. S., et al. 2019, *A&A*, 632, A30
- Trujillo Bueno, J., & Landi Degl'Innocenti, E. 1997, *ApJ*, 482, L183
- Sabin, L., Wade, G. A., & Lèbre, A. 2015, *MNRAS*, 446, 1988
- Scargle, J. D. 1982, *ApJ*, 263, 835
- Stenflo, J. O., & Keller, C. U. 1997, *A&A*, 321, 927
- Waters, L. B. F. M., Waelkens, C., Mayor, M., et al. 1993, *AAP*, 269, 242